

SKIN LAYER OF BiFeO₃ SINGLE CRYSTALS

Xavi Martí^{1,†}, Julia Herrero-Albillos², Pilar Ferrer^{3,4}, Vaclav Holy¹, Marin Alexe⁵,
Gustau Catalan^{6,7‡}

¹ Charles University in Prague, Faculty of Mathematics and Physics, Czech Republic

² Helmholtz-Zentrum Berlin für Materialien und Energie GmbH, Albert-Einstein-Str. 15, 12489 Berlin, Germany

³ SpLine (BM25), ESRF, Grenoble, France .

⁴ Instituto de Ciencia de Materiales de Madrid ICMM-CSIC, Madrid, Spain.

⁵ Max Planck Institute of Microstructure Physics, Weinberg 2, 06120 Halle, Germany

⁶ Institut Català de Recerca i Estudis Avançats (ICREA), Catalunya, Spain

⁷ Centre d'Investigacions en Nanociència i Nanotecnologia (CIN2), CSIC-ICN, Campus Bellaterra, 08193 Barcelona, Spain

Abstract

A surface layer (“skin”) that is functionally and structurally different from the bulk was found in single crystals of BiFeO₃. Impedance analysis indicates that a previously reported phase transition at $T^* \sim 275 \pm 5^\circ\text{C}$ is confined within the surface of BiFeO₃, and grazing incidence x-ray diffraction confirms that the skin’s out of plane lattice parameter increases sharply at T^* , while the bulk of the sample remains completely unchanged. Meanwhile, the room temperature symmetry of the surface is found to be lower than that of the interior: the out-of-plane lattice parameter is contracted and therefore the out-of-plane component of the polarization is reduced. The distinct structure of the surface will affect samples with large surface to volume ratios such as fine grained ceramics and thin films, and should be particularly relevant for devices that rely on interfacial coupling.

[†] xavi.mr@gmail.com

[‡] gustau.catalan@cin2.es

Bismuth ferrite, BiFeO_3 , has become the cornerstone of magnetoelectric multiferroic research, thanks to its high ferroelectric and magnetic ordering temperatures, large ferroelectric polarization, and strong coupling between polarization and magnetic easy plane, all of which are potentially useful for devices [1, 2, 3]. And, yet, the phase diagram of this archetypal material is still an enigma, with a large (and growing) number of structural and/or functional anomalies reported as a function of temperature that may or may not signal the existence of phase transitions (see Ref. [3] for a critical review of some of them). Another unaddressed issue concerns the existence or otherwise of a surface layer (a “skin”) in BiFeO_3 . Notice that several important perovskites (e.g. SrTiO_3 [7,8], BaTiO_3 [9] or relaxor $\text{Pb}(\text{Mg}_{1/3}\text{Nb}_{2/3})\text{O}_3$ [10]) are known to have surface layers that are structurally different from the interior of the crystal. The existence of a surface layer with different symmetry in BiFeO_3 would not be surprising; recent work by Dieguez *et al.* [11] has shown that there is a plethora of different structural phases within just 100 meV of the ground state of BiFeO_3 , an energy gap comparable to surface relaxation energies of perovskites [12, 13].

The problem of the nature of the surface may be connected to the problem of the unexplained phase transitions, and may in fact account for the most intriguing aspect of these anomalies, which is that their observation depends on the experimental technique used. For example, back-scattering Raman experiments show strong phonon softening at $T^*=270^\circ\text{C}$ [4], and yet this apparent phase transition was completely undetected by either birefringence [5] or neutron studies [6]. If the transition at T^* were confined within the surface, this would explain why it is observed in backscattering Raman, which is a surface-sensitive probe, but not in transmission (neutron and birefringence) experiments, which are bulk-sensitive techniques. Aside from these fundamental questions, characterizing the skin of BiFeO_3 is also crucial from an applied point of view, because the spintronic devices proposed for this material are based on interfacial interactions, such as exchange bias between its surface (its skin) and contiguous ferromagnetic layers [2, 14, 15].

Aiming to unravel these issues, we have investigated the structural and dielectric properties of the skin layer of BiFeO_3 single crystals as a function of temperature, with techniques allowing a tuneable information depth. Impedance analysis indicates that the reported anomaly at T^* indeed corresponds to a phase transition localized only at the interface, while grazing incidence x-ray diffraction confirms that the lattice spacing of the surface changes abruptly at T^* , with the bulk remaining unchanged. Such completely decoupled and localized phase transitions are quite unprecedented, but they may not be unique: we note that, at low temperatures, there are other unexplained anomalies in this material [16]. Meanwhile, at room temperature the skin of BiFeO_3 is found to have a contracted out-of-plane lattice parameter, consistent with a surface tilting of the polarization towards the horizontal (in-plane) direction. These results are evidence that the surface of BiFeO_3 is different from its interior, both structurally and functionally.

Following the method proposed by Kubel and Schmid [17], rosette-like crystals, as described by Burnett *et al.* [18], were obtained. The sample used for x-ray investigations was optically polished using sandpaper and diamond paste. Finally, in order to minimize the mechanically damaged surface layer whilst preserving its smoothness, a 30 minute chemical-mechanical polishing using silica slurry (Syton SF1;

Logitech) was employed. The final local RMS roughness was better than 0.8 nm, as determined by atomic force microscopy. The crystals grow with the perovskite pseudocubic $\langle 001 \rangle$ axis out of plane. Ferroelectric/ferroelastic domains are clearly observable using birefringence (see figure 1). The quadrant arrangement is consistent with the polar vector pointing alternately the four diagonals of the perovskite unit cell, though the existence of actual ferroelectric flux closure cannot be verified by birefringence alone. We parenthetically note that this would be a rare example of macroscopically observable ferroelectric closure quadrant, with previous examples limited to nanoscopically engineered domains in thin films [19]. Dendritic crystals with (110) planes parallel to the surface were also made by Tabares-Muñoz and Schmid [20-22], and their electrical properties were characterised. The surface transition was seen in both sets of crystals.

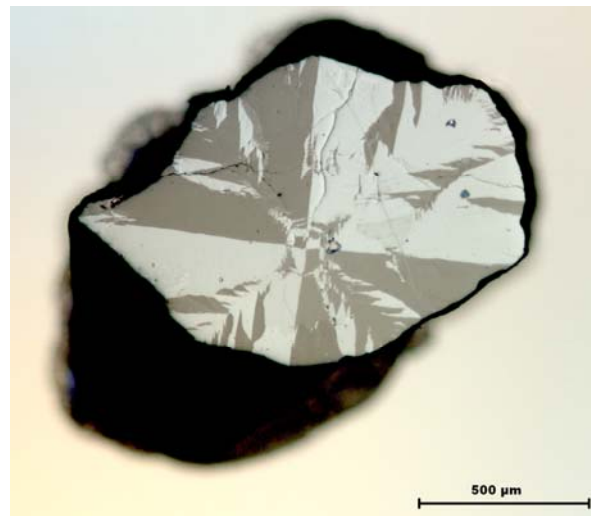


Figure 1 Polarized optical microscopy viewgraph of a mirror-polished single crystal of BFO with habitus parallel to $\langle 001 \rangle_{\text{pseudocubic}}$, showing a quadrant-like arrangement of the four types of ferroelastic domain present in the sample.

The ac impedance of a (110) crystal, measured using an Agilent impedance analyzer (model 4294A), is shown in Figure 2. The electrodes were sputtered gold, with Pt wires attached to them using silver paste. The capacitive impedance shows Maxwell-Wagner behaviour [23], typical of a material with two lossy dielectric components in series, corresponding to the bulk and the interfacial regions [24, 25]. The giant and frequency-dependent increase in capacitance is due to the bulk of the crystal becoming more conducting than the interface (the large loss at high temperature and/or low frequency indicate that the impedance is dominated by charge transport); as the voltage is then mostly dropped on a very thin interfacial region, there is a large increase in *apparent* capacitance [25]. The key observation here is that, for the low frequency data (where interfacial capacitance is probed), there is a small peak whose temperature ($T^* = 272 \text{ }^\circ\text{C}$) is frequency-independent (figure 2). The fact that the position of T^* is frequency-independent indicates that it is not a dynamic effect and is therefore consistent with a true phase transition. On the other hand, the fact that there is no anomaly in the high frequency curves (where bulk capacitance dominates) implies [26] that the bulk of the crystal is not undergoing any phase transition. The T^* peak therefore corresponds to a phase transition confined within the skin of the crystal.

The T^* anomaly has also been observed in ceramics, which have a bigger surface to volume ratio, using Raman in backscattering geometry, and a faint trace is even noticeable in reflection-mode x-ray diffraction [4], but the anomaly is absent in optical [5] and neutron [6] transmission experiments. One thus notices that the anomaly is best evidenced by techniques more sensitive to the surface rather than the bulk. On these grounds, X-ray diffraction at grazing incidence angle (GID) is a very convenient technique to track the eventual structural changes, with an information depth selected at will from few unit cells to several hundreds of microns by changing the incidence angle [27]. We therefore used GID to characterize the surface layer of BiFeO_3 . The GID experiments were carried out at a fixed wavelength of 0.826 \AA on a six-circle diffractometer and a point scintillation detector at SpLine beamline (BM25B), ESRF, Grenoble, France [28]. The sample was placed on a heating stage covered with an airtight capton housing filled with 1 bar of pure oxygen in order to prevent the formation of oxygen vacancies at high temperature. The temperature range of this study is $25^\circ\text{C} - 400^\circ\text{C}$.

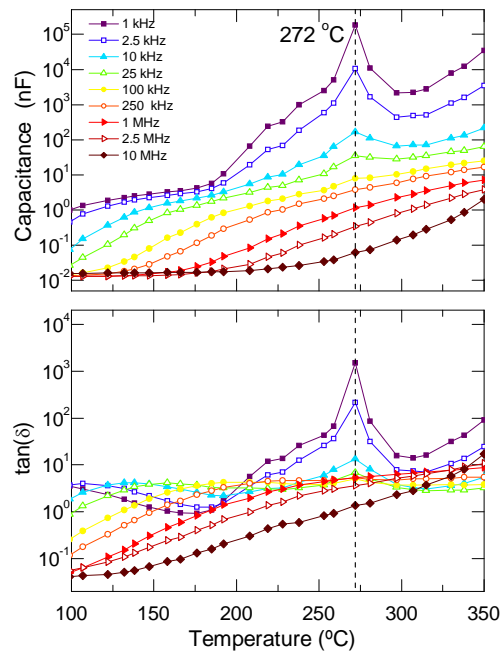


Figure 2. The impedance spectroscopy shows a peak at $T^*=272^\circ\text{C}$ in the low frequency, high capacitance region of the spectrum; this peak is absent from the high frequency data, signalling that the phase transition is confined to the interfacial region.

Before starting the diffraction measurements we have checked the quality of the surface by measuring the x-ray specular reflection. From the reflectivity data we determined the root-mean square roughness of the substrate to $(1.3 \pm 0.1) \text{ nm}$ and the BiFeO_3 density to $(9.15 \pm 0.05) \text{ gcm}^{-3}$; these values are close to the directly measured roughness of 0.8 nm (using atomic force microscopy) and theoretical chemical density of 8.34 g/cm^3 . The critical angle of total external reflection is (0.211 ± 0.005) degrees for the photon energy used at the synchrotron.

We first show the room temperature evidence of a skin layer, based on X-ray diffraction measurements performed on a crystal with (001) planes parallel to the surface. Fig. 3 shows reciprocal space maps around the (102) reflection collected while freezing the incidence angle at shallow (0.1°, panel a) and deep (5°, panel b) values, corresponding to a penetration depth of 1 nm and 1 micron, respectively [27]. Due to the presence of ferroelastic domains (rhombohedral crystal structure) as well as mosaicity in the BiFeO₃ crystals, we used a pseudocubic orientation matrix as the most efficient tool to explore the reciprocal space using a base of three perpendicular reciprocal lattice vectors: H, K and L, with L being the direction perpendicular to the crystal surface. The maps in Fig. 3 correspond to a two-dimensional projection of three dimensional collected meshes.

The reciprocal space maps in Fig. 3 evidence all the mentioned features: first, due to the ferroelastic twinning, splitting between the (102) and (0 $\bar{1}$ 2) reflections is observed. Second, there is considerable broadening of the intensity maxima. This spread is due to mosaicity [29], and complicates somewhat the analysis. However, the mosaic blocks are randomly rotated but not deformed, i.e., the actual lattice parameters are independent of mosaic rotation since the mosaic broadening of the diffraction maxima is in the direction perpendicular to the scattering vector. Of relevance here is that for the determination of the (102)-interplanar distances in the skin and in the bulk it is only necessary to collect the lengths, $Q = \sqrt{H^2 + K^2 + L^2}$, of the scattering vector. The point of this analysis is that Q is a unique signature for a given interplanar distance in the crystal, irrespective of the presence and orientation of the twins and mosaic, in analogy with powder diffraction.

In Fig. 3-c we plot the radial distribution of intensities integrated over the angular directions for each shell of constant Q value (i.e., the histogram of the moduli of Q) for the 3-dimensional HKL maps acquired at high and subcritical incidence angles. The histograms confirm there are only two values of Q , as expected for the rhombohedrally distorted perovskite unit cell. Crucially, the comparison between the surface and bulk histograms reveal a very clear shift towards larger Q values in the skin. The increased Q implies smaller lattice spacing. Meanwhile, the skin is expected to be in-plane coherent with the underlying bulk [30], and therefore the reduction of the (102)-interplanar spacing implies a contraction of the out-of-plane lattice parameter. From the difference ΔL between diffraction maxima at small and large incidence angles we can estimate the skin's out-of-plane lattice contraction:

$$\frac{c_{\text{skin}} - c_{\text{bulk}}}{c_{\text{bulk}}} \approx -\frac{\Delta L}{L} \approx -(4 \pm 0.5) \times 10^{-3}. \text{ This contraction implies a reduction of the out-}$$

of-plane component of the polarization. However, the polar vector in BiFeO₃ is known to be rigid, so that changes in polarization are achieved by rotation of the polar vector [31], in this case towards the horizontal direction (Figure 3-d). Assuming therefore in-plane coherence and constant modulus of the polarization [31], the distortion angles of the perovskite unit cell were calculated as 89.27° for the out-of-plane angles, smaller than the in-plane bulk value (89.56°). The surface symmetry is therefore reduced to triclinic. We parenthetically notice that the lattice contraction (0.4%) is of the same order as that achievable by epitaxial growth of thin films, suggesting that the strain-temperature phase diagram of BiFeO₃ should incorporate intrinsic skin effects.

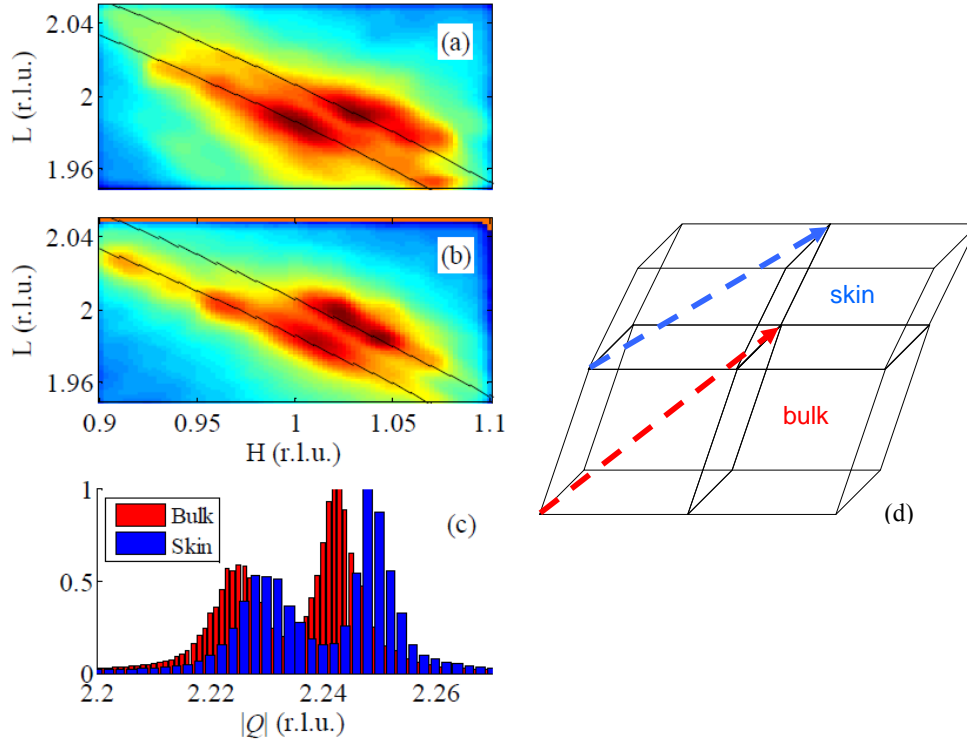


Figure 3: Reciprocal space map around of the (102) reflection measured at (a) deep angle and (b) grazing incidence showing two peaks corresponding to the two diagonals of the ferroelastic domains. The oblique black lines mark the Q values corresponding to the two diagonals of the rhombohedrally distorted unit cell in the bulk; one can see the skin's shift of the intensity maxima away from the black lines in panel (b). (c) The Q -histogram analysis (see text) reveals more clearly the shift of the grazing incidence data (skin, blue) towards bigger scattering vectors (smaller lattice parameters) as compared to the interior of the crystal (bulk, red), thus evidencing the existence of a skin layer contraction in BiFeO_3 . (d) Schematic (exaggerated) of the skin's distortion: the out-of-plane lattice contraction combined with the in-plane coherence and the known rigidity of the polar vector [31] results in a rotation of the polarization towards the surface of the crystal.

Now we turn to the anomaly observed in the impedance spectrum and its connection with the existence of a skin layer. The temperature dependence of the out-of-plane lattice parameter is shown in figure 4 for large (empty symbols) and small (solid symbols) incident angles, corresponding to large ($\sim 1\mu\text{m}$) and small ($\sim 1\text{nm}$) penetration depths respectively. The difference between the two curves is striking: whereas the deep angle (bulk) curve shows a featureless linear thermal expansion, the curve corresponding to the skin shows a marked anomaly, with negative thermal expansion setting in around 260°C followed by a sharp increase in unit cell volume at 280°C . The structural phase transition is therefore confined within the skin.

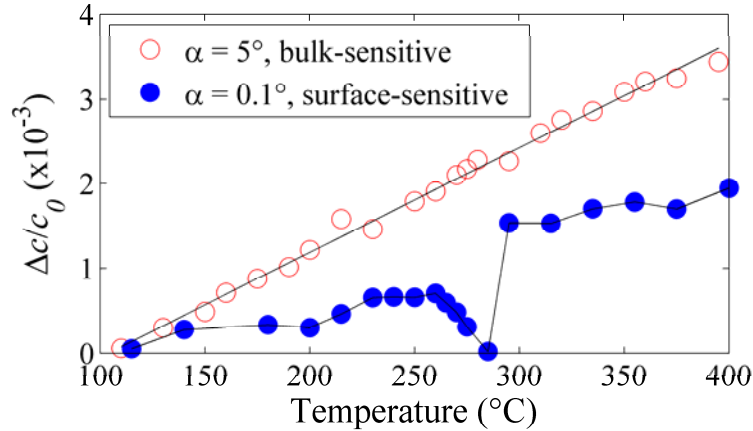


Figure 4. Comparison between the reciprocal thermal expansion at the skin (solid symbols) and inside the crystal (empty symbols) evidencing the local phase transition at T^* in the surface of BiFeO_3 .

In summary, functional (impedance) and structural (grazing incidence diffraction) characterization of BiFeO_3 single crystals indicate the presence of a skin with different properties from those of bulk. The skin has a phase transition at $T^* = 275 \pm 5$ °C, with a sharp structural discontinuity that is not observed inside the crystal. Such decoupled skin transition is quite unprecedented, and is probably facilitated by the richness and relative flatness of the phase diagram of BiFeO_3 [11]. We do not discard that skin effects also participate in other unexplained phase transitions of this material at cryogenic temperatures [3, 16]; two prime candidates are the anomalies at 200K and 140K, which have also been detected by back-scattering Raman [16, 32] but not by neutrons or bulk magnetometric measurements [33].

At room temperature, the Q-histogram method, in analogy with conventional powder diffraction, has allowed the lattice analysis of the of a twinned crystal with mosaicity. The data show unequivocally that the skin's interplanar distances are smaller than the bulk's, implying a rotation of the polarization towards the surface. The polar rotation should also affect also the magnetic and magnetoelectric properties, because the spin cycloid and magnetic easy plane are directly coupled to the polarization [15, 34, 35]. Since BiFeO_3 spintronic devices are based on interfacial coupling [2], the present results will bear on their performance.

We thank Professor Hans Schmid for the loan of one of the crystals used in this study, and for the critical reading of this manuscript. We also thank the SpLine staff for their assistance in using beamline BM25B-SpLine. The financial support of the Spanish Ministerio de Ciencia e Innovación (PI201060E013), Consejo Superior de Investigaciones Científicas (PIE 200960I187) the German Science Foundation (Grant SFB762), and of the EU (Project NAMASTE) is also acknowledged. M. A. and G. C. thank the Lewerhulme trust for the funds that have enabled their collaboration.

References

1. Eerenstein, W., Mathur, N. D. & Scott, J. F., Magnetolectric and multiferroic materials, *Nature* **442**, 759 (2006).
2. H. Bea, M. Gajek, M. Bibes, A. Barthelemy, Spintronics with Multiferroics, *Journal of Physics: Condensed Matter* **20**, 434221 (2008).
3. G. Catalan, J.F. Scott, Physics and Applications of Bismuth Ferrite, *Advanced Materials* **21**, 2463 (2009).
4. R. Haumont, I. A. Kornev, S. Lisenkov, L. Bellaiche, J. Kreisel, and B. Dkhil, Phase stability and structural temperature dependence in powdered multiferroic BiFeO₃, *Phys. Rev. B* **78**, 134108 (2008).
5. J. -P. Rivera, H. Schmid, On the birefringence of magnetoelectric BiFeO₃, *Ferroelectrics* **204**, 23 (1997).
6. P. Fischer, M. Polomska, I. Sosnowska and M. Szymanski, Temperature dependence of the crystal and magnetic structures of BiFeO₃, *J. Phys. C: Solid St. Phys.*, **13**, 1931 (1980).
7. K. Hirota, J. P. Hill, S. M. Shapiro, G. Shirane, Y. Fujii, Neutron- and x-ray scattering study of the two length scales in the critical fluctuations of SrTiO₃, *Phys. Rev. B* **52**, 13195 (1995).
8. S. Ravy, D. Le Bolloc'h, R. Currat, A. Fluerasu, C. Mocuta, and B. Dkhil, SrTiO₃ Displacive Transition Revisited via Coherent X-Ray Diffraction, *Phys. Rev. Lett.* **98**, 105501 (2007).
9. I. A. Luk'yanchuk, A. Schilling, J. M. Gregg, G. Catalan, and J. F. Scott, Origin of ferroelastic domains in free-standing single-crystal ferroelectric films, *Phys. Rev. B* **79**, 144111 (2009).
10. G. Xu, P. M. Gehring, C. Stock, K. Conlon, The anomalous skin effect in single crystal relaxor ferroelectric PZN-x PT and PMN-x PT, *Phase Transitions* **79**, 135 (2006).
11. Oswaldo Diéguez, O.E. González-Vázquez, Jacek C. Wojdel, Jorge Íñiguez, First-principles predictions of low-energy phases of multiferroic BiFeO₃, arXiv:1011.0563 (2010).
12. J. Padilla and D. Vanderbilt, Ab initio study of BaTiO₃ surfaces, *Phys. Rev. B* **56**, 1625 (1997).
13. J. Padilla and David Vanderbilt, Ab-initio study of SrTiO₃ surfaces, *Surf. Sci.* **418**, 64 (1998).
14. J. Dho, X. Qi, H. Kim, J.L. MacManus-Driscoll, M. G. Blamire, "Large Electric Polarization and Exchange Bias in Multiferroic BiFeO₃" *Adv. Mat.* **18**, 1445 (2006).
15. D. Lebeugle, A. Mougin, M. Viret, D. Colson, and L. Ranno, "Electric Field Switching of the Magnetic Anisotropy of a Ferromagnetic Layer Exchange Coupled to the Multiferroic Compound BiFeO₃", *Phys. Rev. Lett.* **103**, 257601 (2009).
16. M.K. Singh, R. Katiyar, and J.F. Scott, "New magnetic phase transitions in BiFeO₃", *J. Phys. Condens. Matter* **20**, 252203 (2008).
17. F. Kubel and H. Schmid, "Growth, twinning and etch figures of ferroelectric/ferroelastic dendritic BiFeO₃ single domain crystals", *J. Cryst. Growth* **129**, 515 (1993).
18. T.L. Burnett, T. P. Comyn, and A. J. Bell, Flux growth of BiFeO₃-PbTiO₃ single crystals, *J. Cryst. Growth* **285**, 156 (2005).

19. N. Balke, S. Choudhury, S. Jesse, M. Huijben, Y. H. Chu, A. P. Baddorf, L. Q. Chen, R. Ramesh & S. V. Kalinin, “Deterministic control of ferroelastic switching in multiferroic materials”, *Nature Nanotech.* **4**, 868 (2009).
20. C. Tabares-Muñoz, PhD thesis, University of Geneva, Switzerland (1986).
21. C. Tabares-Muñoz, J.-P. Rivera, A. Bezings, A. Monnier and H. Schmid, *Jpn. J. Appl. Phys., Part I*, **24**, 1051 (1985).
22. R. Palai, R. S. Katiyar, H. Schmid, P. Tissot, S. J. Clark, J. Robertson, S. A. T. Redfern, G. Catalan, and J. F. Scott, “ β phase and γ - β metal-insulator transition in multiferroic BiFeO_3 ”, *Phys. Rev. B* **77**, 014110 (2008).
23. A. Von Hippel, “Dielectrics and Waves”, Wiley (New York 1954).
24. P. Lunkenheimer, V. Bobnar, A. V. Pronin, A. I. Ritus, A. A. Volkov, and A. Loidl, “Origin of apparent colossal dielectric constants” *Phys. Rev. B* **66**, 052105 (2002).
25. G. Catalan, J. F. Scott, “Magnetolectrics: is CdCr_2S_4 a multiferroic relaxor?” *Nature* **448**, E4-E5 (2007).
26. J. F. Scott, “Dielectric anomalies in nonferroelectric phase-transitions”, *JETP letters* **49**, 233 (1989).
27. U. Pietsch, V. Holy, T. Baumbach, *High-Resolution X-Ray Scattering: from thin films to lateral nanostructures*, Springer-Verlag (New York, 2004).
28. G.R. Castro, “Optical design of the general-purpose Spanish X-ray beamline for absorption and diffraction” *J. Synchrotron Rad.* **5**, 657 (1998).
29. From the angular broadening of the diffraction maxima we can estimate also the mean misorientation of the mosaic blocks: $\Delta\omega = (1.3 \pm 0.3)$ deg.
30. The continuity of the lateral lattice parameter at the bulk-skin interface should cause a continuity of the lateral components of the vector Q , i.e. the lateral coordinates of the maxima of the bulk and the skin phases should have identical H-coordinates. Unfortunately, the uncertainty associated with the mosaic spread in both phases prevents direct confirmation of this continuity relation.
31. H. W. Jang, S. H. Baek, D. Ortiz, C. M. Folkman, R. R. Das, Y. H. Chu, P. Shafer, J. X. Zhang, S. Choudhury, V. Vaithyanathan, Y. B. Chen, D. A. Felker, M. D. Biegalski, M. S. Rzchowski, X. Q. Pan, D. G. Schlom, L. Q. Chen, R. Ramesh, and C. B. Eom, “Strain-Induced Polarization Rotation in Epitaxial (001) BiFeO_3 Thin Films”, *Phys. Rev. Lett.* **101**, 107602 (2008).
32. M. Cazayous, Y. Gallais, A. Sacuto, R. de Sousa, D. Lebeugle, and D. Colson, “Possible Observation of Cycloidal Electromagnons in BiFeO_3 ”, *Phys. Rev. Lett.* **101**, 037601 (2008).
33. J. Herrero-Albillos, G. Catalan, J. A. Rodriguez-Velamazan, M. Viret, D. Colson and J. F. Scott, “Neutron diffraction study of the BiFeO_3 spin cycloid at low temperature” *J. of Phys. Cond. Mat.* **22**, 256001 (2010).
34. T. Zhao, A. Scholl, F. Zavaliche, K. Lee, M. Barry, A. Doran, M. P. Cruz, Y. H. Chu, C. Ederer, N. A. Spaldin, R. R. Das, D. M. Kim, S. H. Baek, C. B. Eom and R. Ramesh, “Electrical control of antiferromagnetic domains in multiferroic BiFeO_3 films at room temperature”, *Nature Materials* **5**, 823 (2006)
35. D. Lebeugle, D. Colson, A. Forget, M. Viret, A. M. Bataille, and A. Gukasov, “Electric-Field-Induced Spin Flop in BiFeO_3 Single Crystals at Room Temperature” *Phys. Rev. Lett.* **100**, 227602 (2008).